# ZYG-9, A *Caenorhabditis elegans* Protein Required for Microtubule Organization and Function, Is a Component of Meiotic and Mitotic Spindle Poles

**Lisa R. Matthews,* Philip Carter,* Danielle Thierry-Mieg,‡ and Ken Kemphues***

*Section of Genetics and Development, Cornell University, Ithaca, New York 14850; and ‡Centre de Recherches de Biochimie Macromoléculaire du Centre National de la Recherche Scientifique, 34293 Montpellier, France

***Abstract.*** We describe the molecular characterization of *zyg-9*, a maternally acting gene essential for microtubule organization and function in early *Caenorhabditis elegans* embryos. Defects in *zyg-9* mutants suggest that the *zyg-9* product functions in the organization of the meiotic spindle and the formation of long microtubules. One-cell *zyg-9* embryos exhibit both meiotic and mitotic spindle defects. Meiotic spindles are disorganized, pronuclear migration fails, and the mitotic apparatus forms at the posterior, orients incorrectly, and contains unusually short microtubules. We find that *zyg-9* encodes a component of the meiotic and mitotic spindle poles. In addition to the strong staining of spindle poles, we consistently detect staining in the region of the kinetochore microtubules at metaphase and early anaphase in mitotic spindles. The ZYG-9 signal at the mitotic centrosomes is not reduced by nocodazole treatment, indicating that ZYG-9 localization to the mitotic centrosomes is not dependent upon long astral microtubules. Interestingly, in embryos lacking an organized meiotic spindle, produced either by nocodazole treatment or mutations in the *mei-1* gene, ZYG-9 forms a halo around the meiotic chromosomes. The protein sequence shows partial similarity to a small set of proteins that also localize to spindle poles, suggesting a common activity of the proteins.



During the cell cycle, dramatic changes occur in the organization and dynamic properties of microtubules. The extensive interphase network of microtubules rapidly disassembles and is replaced by the spindle apparatus, a bipolar array of shorter, more dynamic microtubules. Although it has been demonstrated that changes in microtubule dynamics are mediated by cyclin A– and cyclin B–dependent kinases (Verde et al., 1992), the precise mechanisms by which these changes are regulated in response to cell cycle–dependent cues are not yet clear.

The changes in the organization and dynamic properties of microtubules in early embryos are especially striking. In organisms such as *Caenorhabditis elegans* and *Xenopus laevis,* meiotic and mitotic spindles form in the same cytoplasm within minutes of one another. In addition, the large size of early blastomeres and rapid rate of cell divisions requires timely assembly and disassembly of unusually long microtubules (Stewart-Savage and Grey, 1982).

How are the organization and dynamic properties of microtubules regulated during early embryogenesis? *Xenopus* egg extracts have made possible the identification and analysis of microtubule-associated proteins with likely roles in regulating microtubule dynamics (Gard and Kirschner, 1987; Andersen et al., 1994; Vasquez et al., 1994; Andersen and Karsenti, 1997). One of these proteins, XMAP215, may play a particularly important role in meeting the demands of early embryos. XMAP215 is expressed primarily in oocytes, eggs, and early embryos and is a component of the spindle poles (Gard and Kirschner, 1987; Gard et al., 1995). In vitro, XMAP215 increases the rate of microtubule turnover and promotes the formation of long microtubules by increasing the rate of microtubule polymerization, particularly at the plus end (Gard and Kirschner, 1987; Vasquez et al., 1994). Evidence suggests that XMAP215 plays a primary role in the increase in the dynamic properties of microtubules between oocyte maturation and fertilization, and in facilitating the rapid assembly and reorganization of microtubules in the large early blastomeres after fertilization (Gard and Kirschner, 1987; Vasquez et al., 1994).

Genetic analysis provides another method for identifying proteins with roles in regulating microtubule organization in early embryos. In *C. elegans,* maternal effect mutations in two genes, *mei-1* and *zyg-9*, affect the organization of microtubules in one-cell embryos. The *mei-1* gene encodes an ATPase required for meiotic spindle formation that appears to restrict the length of meiotic spindle micro-

Address all correspondence to Ken Kemphues, Section of Genetics and Development, 101 Biotechnology Bldg., Cornell University, Ithaca, NY 14853. Tel.: (607) 254-4805. Fax: (607) 255-6249. E-mail: kjk1@cornell.edu

tubules (Mains et al., 1990*b*; Clark-Maguire and Mains, 1994*a*,*b*). The *zyg-9* gene is required for meiotic spindle assembly and for the formation of the exceptionally long microtubules in the mitotic spindle apparatus of early embryos (Albertson, 1984; Kemphues et al., 1986). During meiosis, *zyg-9* mutant embryos exhibit disorganized spindles and numerous cytoplasmic clusters of short microtubules (Kemphues et al., 1986). Subsequently, pronuclear migration fails as does the migration and rotation of the centrosome–nuclear complex. A mitotic spindle apparatus containing unusually short microtubules then forms in the posterior of the embryos, perpendicular to its normal position. The first cleavage division is abnormal and the embryos arrest after several cell divisions, presumably due to aneuploidy (Wood et al., 1980). Temperature shift experiments suggest that maternal *zyg-9* is essential for viability during the first cell cycle, and that there is a less stringent requirement for this gene product until the onset of gastrulation (Kemphues et al., 1986; Mains et al., 1990*a*). *zyg-9* activity is dispensable after gastrulation. The possibility that the *zyg-9* product is involved in microtubule function is supported by observations that treatment of early embryos with the microtubule destabilizing drug nocodazole mimics *zyg-9* defects (Albertson, 1984).

We demonstrate here that ZYG-9 is a component of the meiotic and mitotic spindle poles, is a transient component of the central spindle, and exhibits sequence similarity to a small group of proteins that also localize to spindle poles and regulate microtubule behavior.

## Materials and Methods

### Strains and Alleles

The N2 Bristol strain was used as the wild-type strain. The *zyg-9* alleles used in these analyses were the ethyl methane sulfonate–induced alleles, *b244*ts (Wood et al., 1980), *b279*, *b288*ts, *b301*, *b307*, *ct10*, and *it3* (Kemphues et al., 1988), which were isolated in screens for maternal effect lethal mutations, the *zyg-9* alleles *it63* and *it64*, induced in the *mut-2* mutator strain TR679 (Collins et al., 1989), and *it152,* isolated from a strain carrying the mutator-induced mutation *sqt-1* (*sc114)*. Other mutations used were *sqt-1(sc114)*, *dpy-10*(*e128*), *unc-4*(*e120*), *zyg-11*(*b272*), *rol-6*(*e187*), *mnC dpy-10 unc-52*, and fP1, a new Tc1 polymorphism closely linked to *zyg-9* in the strain *zyg-9(it152) sqt-1(sc114)*.

### Genetic Analysis

*zyg-9* was mapped relative to the cloned markers *zyg-11*, fP1, and *rol-6* on linkage group (LG) II. The strain *dpy-10 zyg-11 rol-6*/fP1 *zyg-9 (it152)* was constructed and a standard multifactor recombination analysis was performed except that the presence of the fP1 marker was detected using the single worm PCR method of Williams et al. (1992). The recombinants obtained (290 between *dpy-10* and *zyg-11*, 35 between *zyg-11* and fP1, 5 between fP1 and *zyg-9,* and 62 between *zyg-9* and *rol-6*) revealed that *zyg-9* was located at 0.7 m.u. on the chromosome II physical map, ~0.009 map units (m.u.) to the left of fP1. This corresponds to a physical distance of ~24 kb, assuming a distance of 320 kb between fP1 and *rol-6* (Waterston and Sulston, 1995).

### Germline Transformation Rescue of zyg-9

K07D6, C45G11, or C28G11 cosmid DNA (15–40 ng/μl) were mixed with plasmid DNA carrying the dominant marker, *rol-6*(*su1006*) (200–300 ng/μl), and then injected into the distal arms of both gonads of KK44 [*zyg-9* (*b279*)*unc-4*/*mnC1* II] using the protocol of Mello et al. (1991). Rol non-Unc progeny were picked to separate plates to identify germline transformants. To assay for rescue of *zyg-9*, Unc Rol and Unc non-Rol segregants from germline-transformed lines were tested for the production of viable progeny.

### Molecular Analysis

Southern blot analyses of wild-type (N2) and *zyg-9* mutant DNAs were performed according to standard protocols (Ausubel et al., 1995). Genomic DNA was prepared using the Puregene kit (Gentra Systems, Research Triangle Park, NC). Allele-specific DNA polymorphisms were detected using C28G11 cosmid DNA and yk28d8 cDNA as probes (The yk28d8 cDNA clone was a generous gift from Y. Kohara, National Institute of Genetics, Mishima, Japan). An open reading frame in the region of the gene-specific polymorphisms was identified using the genefinder program of ACeDB (Durbin and Thierry-Mieg, 1991). Additional cDNAs were isolated by screening a λgt11 mixed stage cDNA library (Okkema and Fire, 1994) according to standard protocols (Ausubel et al., 1995) using the yk28d8 cDNA as a probe. The largest clone, PO12.3, was used for subsequent analyses.

### RNA Interference

Antisense RNA corresponding to the cDNA yk28d8 was prepared as described by Guo and Kemphues (1995). Antisense RNA (~1 μg/μl) was injected in the gonads of wild-type hermaphrodites as described above. Injected animals were picked to individual plates and scored for embryonic lethality 18 h after injection. Individual one-cell embryos were cut from injected animals, mounted on 5% agar pads for microscopy, and then videotaped to observe embryonic phenotypes during the first cell cycle.

### Identification of the 5′ End of the zyg-9 Transcript and Sequence Analysis

The sequences of the *zyg-9* cDNA PO12.3 were obtained using the dideoxy chain termination method (Sanger et al., 1977). The PO12.3 subclones were sequenced by the Cornell University Biotechnology program Automatic Sequencing Facility (Ithaca, NY). The 5′ end of the *zyg-9* transcript was determined by PCR using the −300 primer in the PO12.3 cDNA sequence (5′GCGAAAGAAGAGAATTTG3′) and the SL1 primer (5′GGTTTAATTACCCAAGTTTGAG3′) containing the SL1 spliced leader sequence. DNA sequences were analyzed using the BLAST program (Altschul et al., 1990) and the Lasergene suite of programs (DNAstar, Inc., Madison, WI).

### Northern Analysis

Northern blots containing poly A mRNA isolated from gravid wild-type worms were prepared according to standard protocols (Ausubel et al., 1995) and probed with the cDNA yk28d8.

### Preparation of ZYG-9 Polyclonal Antibodies

Fusion protein containing the carboxy-terminal 462 amino acids of the ZYG-9 protein was prepared for polyclonal antibody production. A fragment containing 1,385 base pairs from the 3′ end of the *zyg-9* cDNA was cloned into the expression vector QE30 (QIAGEN, Inc., Santa Clarita, CA). ZYG-9–6HIS fusion proteins were expressed in bacteria, inclusion bodies were isolated (Harlow and Lane, 1988), and then the expected 51-kD protein was purified by SDS-PAGE followed by electroelution and dialysis. Rabbit polyclonal antibodies were generated at the Cornell Research Animal Resources Facility (Ithaca, NY). ZYG-9–specific antibodies were purified from crude serum by column chromatography using ZYG-9 fusion protein coupled to CNBr-activated Sepharose 6MB beads (Pharmacia Biotech., Inc., Piscataway, NJ).

### Western Blot Analyses

The specificity of purified antibodies for endogenous ZYG-9 protein was assayed by Western blot analysis. Proteins were prepared from embryos by picking 150 gravid adults into $dH_2O$. Animals were washed and transferred to 20 μl of $dH_2O$. 180 μl of a solution of four parts 0.66 M KOH to one part commercial bleach was added to each sample. After worms dissolved (~3 min), samples were spun at 6,000 rpm for 1 min to pellet the embryos. Embryos were washed twice with 200 μl $dH_2O$, resuspended in 20 μl of sample buffer, boiled for 1 min, and then homogenized (100 strokes) with the narrow end of a Pasteur pipette that had been closed and

rounded by heating. Samples were then boiled an additional 3 min. Proteins were resolved by SDS-PAGE, transferred to Immobilon membranes (Millipore Corp., Waters Chromatography, Milford, MA) and probed with purified antiserum. Antibodies were detected using the enhanced chemiluminescence protein detection kit (Amersham Pharmacia Biotech., Inc., Piscataway, NJ).

### *Immunolocalization of ZYG-9 Protein in Embryos*

Embryos were stained according to the protocol of Albertson (1984) with minor modifications. Adult worms were washed in $dH_2O$, resuspended in PBS, and then transferred with 7–10-μl drops of PBS to polylysine-coated slides. Worms were cut open at the vulva to release embryos, covered with a coverslip, and then frozen immediately on dry ice. Coverslips were removed from frozen slides using a razor blade. Slides were immediately immersed in MeOH (−20°C) for 15 min and then transferred to PBS at room temperature for 5 min. Fixed embryos were incubated in 30 μl of goat serum for 1 h at room temperature. Goat serum was removed and replaced by 10 μl of affinity-purified anti–ZYG-9 antibodies diluted 1:50 in PBS or by mouse monoclonal anti-*Drosophila* α-tubulin antibodies (4A-1, gift of M. Fuller, Stanford University, Stanford, CA) diluted 1:40 in PBS. Slides were incubated in a moist chamber at room temperature for 1 h and then washed for 10 min in PBS-T (1× PBS, 0.5% Tween [Sigma Chemical Co., St. Louis, MO]) followed by two 10-min washes in PBS. 30 μl of secondary antibody (diluted 1:100 in PBS) was added and slides were incubated at room temperature for 1 h. Slides were then washed in PBS-T for 10 min followed by 10 min in PBS; 1 μg/ml of 4′,6-diamidino-3-phenylindole dihydrochloride (DAPI),[1] 10 min in PBS-T, and then 10 min in PBS. Coverslips were mounted with Vectashield (Vector Labs Inc., Burlingame, CA) to decrease photobleaching.

### *Microtubule Disruption*

To disrupt microtubules in embryos before fixation, a protocol adapted from the laboratory of P. Mains (University of Calgary, Calgary, Canada) was used. Embryos were cut out of gravid hermaphrodites in PBS containing 30 μg/ml nocodazole (Sigma Chemical Co.) as described above. Coverslips were placed over embryos and gentle pressure was applied to break the eggshells. Slides were incubated at room temperature for 12 min and then frozen and fixed as described above.

## *Results*

### *Molecular Cloning of zyg-9*

Previous genetic mapping studies placed *zyg-9* at the center of LG II between the genetic markers *zyg-11* and *rol-6* (Kemphues et al., 1988) and to the right of the deficiency *mnDf 104*, an interval of ~0.18 m.u. We further mapped *zyg-9* within this interval using the physical marker fP1, a transposable element closely linked to the *zyg-9* allele, *it152*. This additional mapping data placed *zyg-9* 0.11 m.u. to the left of *rol-6*, ~24 kb to the right of the fP1 marker. These results indicated that *zyg-9* was located within the region covered by the cosmids K07D6, C45G11, and C28G11 (Fig. 1).

To identify the location of the *zyg-9* gene, we tested whether any one of these three cosmids could rescue *zyg-9* mutants. Germline transformants were generated according to the protocol of Mello et al. (1991) as described in Materials and Methods. We were able to rescue *zyg-9(b279)* animals only with the cosmid C28G11. 4 out of 17 C28G11 lines produced a small number of fertile homozygous *zyg-9* transformants (Rol Unc) (Table I). Fertile animals produced between 1 and 10 progeny. Most of these progeny arrested as L1 larvae, but a few developed to adults that produced equally low numbers of viable progeny.

1. *Abbreviation used in this paper*: DAPI, 4′,6-diamidino-3-phenylindole dihydrochloride.

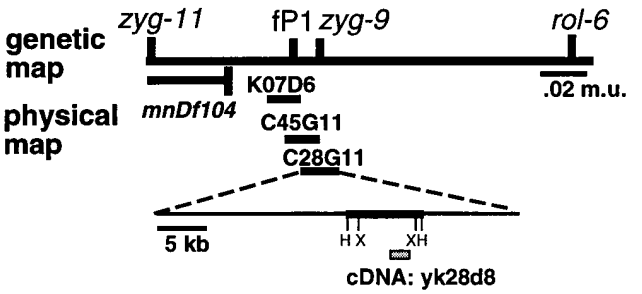


*Figure 1.* Map position of *zyg-9*. The top line shows a portion of the genetic map of linkage group II giving relative positions of the relevant markers. *zyg-9* maps 0.009 m.u. or ~24 kb to the right of the fP1 insertion site which is cloned in cosmid K07D6. The positions of K07D6, C45G11, and C28G11 and the right end of the deletion *mnDf104* are indicated. The locations of the *zyg-9* gene and partial cDNA yk28d8 on C28G11 is indicated below with relevant HindIII and XhoI sites marked.

Three lines of evidence suggested that the weak fertility of the *zyg-9* C28G11 transformants corresponded to rescue. First, the fertility of these correlated with the presence of injected DNA. All fertile homozygous *zyg-9* animals analyzed were phenotypically Rol-6, whereas all of the homozygous *zyg-9* non-Rol segregants from the same lines produced only dead embryos (Table I, *columns 3* and *4*). Second, it is unlikely that the low level of fertility of these transformants was the result of "leakiness" of the *b279* allele because none of the 650 *b279* homozygous progeny from uninjected animals were fertile (Table I, *row 5*). Finally, injection of the pRF4 plasmid alone was not responsible for the observed fertility, as none of 117 *b279* homozygous transformants carrying only pRF4 DNA were fertile (Table I, *row 4*). Together, these results suggest that the *zyg-9* gene is contained within the cosmid C28G11 sequence.

To further test this possibility, we analyzed the *zyg-9* mutants *it64* and *it152*, both isolated in mutator backgrounds, for the presence of restriction fragment length polymorphisms in the region covered by the cosmid C28G11. Using this cosmid as a probe in Southern blot analyses, we detected polymorphisms within a 7.7-kb HindIII fragment in both alleles (data not shown).

Using the published DNA sequence from this region (Waterston and Sulston, 1995) and the genefinder program of ACeDB, three predicted open reading frames were identified within this 7.7-kb HindIII fragment. A 1.6-kb cDNA, yk28d8, corresponding to one of these open read-

*Table 1. Analysis of Transformed Lines*

| DNA-injected* | Number of transformed lines | Fertility of homozygous *zyg-9* transformants (Rol Unc) | Fertility of homozygous *zyg-9* non-Rol segregants |
|---|---|---|---|
| C28G11 | 17‡ | 15/611 | 0/190 |
| K07D6 | 10 | 0/250 | — |
| C45G11 | 8 | 0/200 | — |
| pRF4 alone | 1 | 0/117 | — |
| None | — | — | 0/650 |

*All cosmids were coinjected with plasmid pRF4 carrying a dominant mutation in the *rol-6* gene that confers the Rol-6 phenotype.
‡Only four of these lines gave any rescued animals.

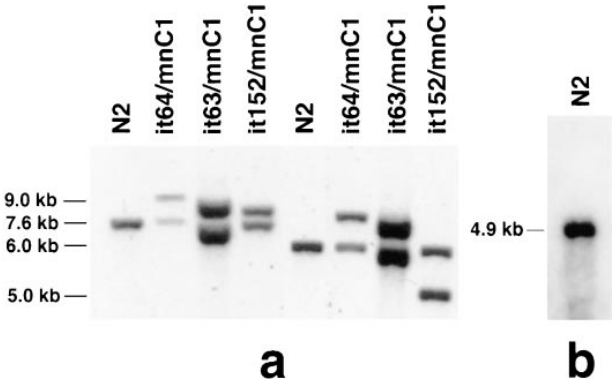


*Figure 2. (a)* Genomic Southern blot analysis of wild-type and *zyg-9* mutants. Genomic DNA from wild type (*N2*) and heterozygous *zyg-9 it63*, *it64*, and *it152* animals was resolved by electrophoresis after digestion with HindIII (*four leftmost lanes*) or XhoI (*four rightmost lanes*), then blotted and probed with yk28d8 cDNA. Novel allele-specific hybridizing bands correlate with the presence of the *zyg-9* mutations. *(b)* Northern blot analysis of mRNA from wild-type (*N2*) adults. Poly A mRNA was isolated, separated by electrophoresis, blotted, and then probed with the yk28d8 cDNA clone. A single band of ~4.9 kb was detected.

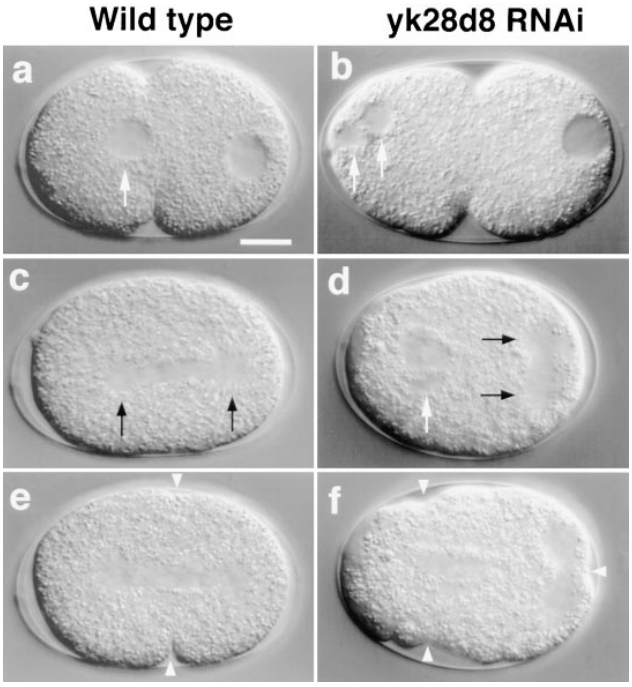


*Figure 3.* Results of RNA interference experiments. Nomarski micrographs of the first cell cycle of a wild-type embryo (*a, c,* and *e)* and embryos from wild-type hermaphrodites injected with yk28d8 antisense RNA *(b, d,* and *f)*. Embryos from the hermaphrodites injected with antisense yk28d8 RNA exhibit defects characteristic of *zyg-9* mutations. These include defects in meiosis II indicated by multiple female pronuclei (*b*, *arrows*), failure of pronuclear migration (*d*, *white arrow;* location of female pronuclei undergoing nuclear envelope breakdown), abnormal size and positioning of the first cleavage spindle (*d*, *black arrows*; centrosomes), and furrows *(f, arrowheads*; positions of cleavage furrows). Bar, ~10 μm.

ing frames, had previously been identified as an expressed sequence tag (Kohara, Y., personal communication). Additional Southern blot analyses using fragments of the yk28d8 cDNA as probes revealed allele-specific novel bands consistent with the possibility that the lesions in the alleles *it64* and *it152*, as well as a third mutator-induced allele, *it63*, are the results of insertions within this transcription unit (Fig. 2 *a*). These observations strongly suggested that the yk28d8 cDNA corresponds to the *zyg-9* gene. We verified this using the method of RNA interference (Rocheleau et al., 1997). This technique has been used successfully to phenocopy numerous *C. elegans* maternal effect mutations (Guo and Kemphues, 1995; Lin et al., 1995; Draper et al., 1996; Hunter and Kenyon, 1996; Mello et al., 1996). Antisense yk28d8 RNA was injected into the gonads of wild-type worms as described in Materials and Methods. The results of this analysis are shown in Table II and Fig. 3.

Animals injected with yk28d8 antisense RNA exhibited *zyg-9*–specific defects. Within 18 h of the injection of antisense yk28d8 RNA, 88% of worms produced more than 50% dead embryos. An analysis of one-cell embryos from injected animals revealed that 70% exhibited defects identical to those observed in the embryos of *zyg-9* mutants. These defects included failure of pronuclear migration, transverse spindle orientation, and a characteristic abnormal first cleavage (Fig. 3). Injection of *par-1* antisense RNA also resulted in a high percentage of embryonic lethality (60%). However, these embryos displayed a Par-1 mutant phenotype that is distinct from that of *zyg-9* (Guo and Kemphues, 1995). Taken together, the rescue of *zyg-9* by the cosmid C28G11, the identification of allele-specific polymorphisms, and RNA interference phenocopy allows us to conclude that the yk28d8 cDNA corresponds to the *zyg-9* gene.

*Table II. Analysis of Animals Injected with Antisense yk28d8 RNA*

| Antisense RNA template | Number of worms injected | Number that produce >50% dead embryos | One-cell embryos videotaped | Embryos showing gene-specific phenocopy |
|---|---|---|---|---|
| yk28d8 | 20 | 18 | 13 | 9 |
| *par-1* | 10 | 6 | 1 | 1 |
| None | 20 | 0 | — | — |

Northern blot analyses revealed that the 1.6-kb yk28d8 cDNA hybridized to a message of ~4.9 kb in wild-type worms (refer to Fig. 2 *b*). To identify the full-length *zyg-9* transcript, we screened a λgt11 cDNA library derived from mixed stage animals (Okkema and Fire, 1994) using the yk28d8 cDNA as a probe. A clone of 4,509 base pairs, PO12.3, was subcloned and sequenced. The sequence of the missing 5′ end of the message was determined as described in Materials and Methods. The 5′ end of the *zyg-9* transcript is transspliced to the SL1 leader three base pairs upstream of the initiating ATG. The complete ZYG-9 sequence has been submitted (EMBL/GenBank/DDBJ accession number AF035197).

### *ZYG-9 Is Similar to Proteins in Yeast and in Humans*

Database searches for proteins similar to the predicted ZYG-9 sequence revealed similarity to the human protein

ch-TOG and, to a lesser extent, two yeast proteins: *Schizosaccharomyces pombe* p93$^{Dis1}$ and *Saccharomyces cerevisiae* Stu2p. ch-TOG is the product of a gene that is overexpressed in colonic and hepatic tumors (Charrasse et al., 1995). The protein associates with microtubules in vitro and is the putative homologue of the *Xenopus* microtubule assembly protein, XMAP215 (Charrasse et al., 1998). The p93$^{Dis1}$ protein is a microtubule-binding protein involved in sister chromatid separation (Nabeshima et al., 1995; Nakaseko et al., 1996; Ohkura et al., 1988). *STU2* was identified as a suppressor of *tub2-423*, a cold-sensitive allele of the β-tubulin gene *TUB2*, and encodes a protein that associates with microtubules in vitro (Wang and Huffaker, 1997).

A schematic representation of the similarities between ZYG-9 and these three proteins is shown in Fig. 4. All four proteins share sequence similarity in a domain of ~220 amino acids. Within this region, ZYG-9 is 35% identical to p93$^{Dis1}$, 31% identical to Stu2p, and 48% identical to ch-TOG. This domain is present in two tandem divergent copies in ZYG-9. These repeats are 52% identical to one another. ZYG-9 and ch-TOG are also 39% identical in a second region of ~280 amino acids.

### *ZYG-9 Is a Component of the Meiotic and Mitotic Spindles Greatly Enriched at the Poles*

To better understand the function of ZYG-9 protein during early development, we determined its subcellular distribution in early embryos by immunofluorescence microscopy using ZYG-9–specific antibodies. Rabbit polyclonal antibodies were raised against a fusion protein containing the carboxy-terminal 462 amino acids of ZYG-9 as described in Materials and Methods. To determine the specificity of the antibodies raised against these fusion proteins, we performed Western blot analyses of proteins from wild-type embryos and embryos from six *zyg-9* mutants using affinity-purified antisera. A single band of 155 kD, the expected size for the ZYG-9 protein, is detected in wild-type embryos (Fig. 5). A band of 155 kD was also detected in the temperature-sensitive *zyg-9* allele *b244*, but not in the four strong alleles, *b301*, *b279*, *it3*, and *it152*, or in the temperature-sensitive allele *b288*.

We studied the distribution of ZYG-9 protein in early embryos by in situ immunofluorescence microscopy. Wild-type and *zyg-9* mutant embryos were fixed and stained with purified polyclonal ZYG-9 antibodies. In certain cases, embryos were also stained for α-tubulin using a mouse monoclonal anti-*Drosophila* α-tubulin antibody (refer to Materials and Methods). We found that ZYG-9 exhibits a dynamic cell cycle-dependent distribution pattern. The protein localizes to the meiotic spindle and spindle poles and to the mitotic centrosomes. In metaphase and early anaphase stages, ZYG-9 can be detected over the central mitotic spindle region as well. During interphase, ZYG-9 protein is distributed throughout the cytoplasm. Specificity of this staining pattern was confirmed by its absence in embryos homozygous for any of three strong *zyg-9* alleles that lacked the 155-kD protein (Figs. 6 *h* and 7 *q*).

### *Meiosis*

The distribution of ZYG-9 is similar in meiosis I and meiosis II spindles. ZYG-9 staining is present throughout the

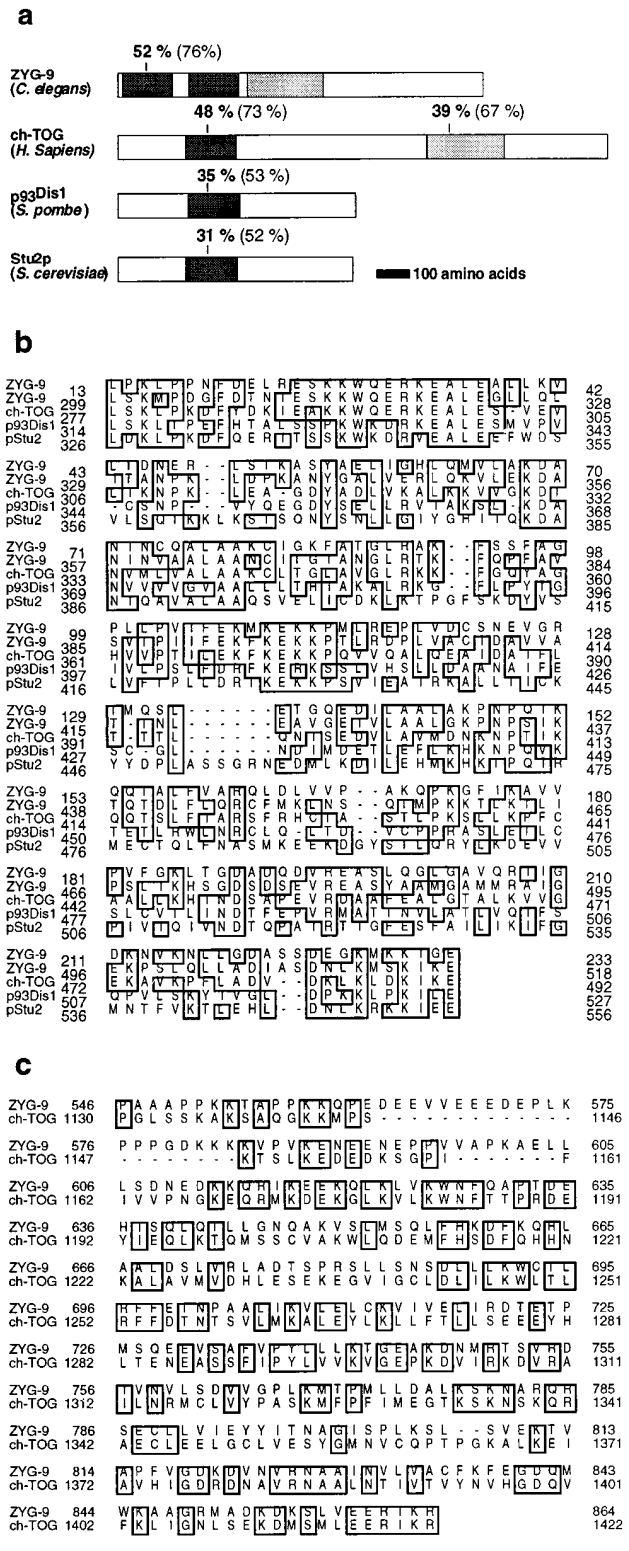


*Figure 4. (a)* Comparison of sequences of ZYG-9, *Homo sapiens* ch-TOG, *S. pombe* p93$^{Dis1}$, and *S. cerevisiae* Stu2p. One domain of ~220 amino acids is conserved in all four proteins (region 1, *black boxes*). This region is present in two divergent copies separated by 65 amino acids in the ZYG-9 protein. A second region of similarity between ZYG-9 and ch-TOG spans ~280 amino acids (region 2, *shaded boxes*). The degree of identity between ZYG-9 and each protein for each domain is indicated in boldface and the degree of similarity (identities + similarities) is indicated in parentheses. Sequence alignments are shown below, with region 1 shown in *b* and region 2 shown in *c*.

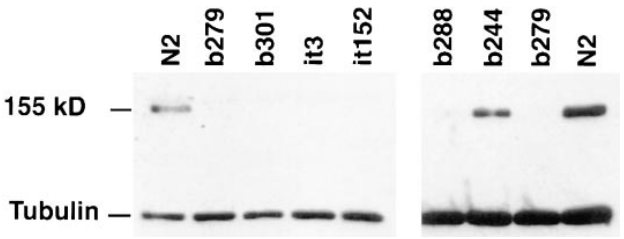


*Figure 5.* Detection of endogenous ZYG-9 protein on Western blots. Extracts from wild-type or *zyg-9* mutant embryos were resolved by SDS-PAGE, blotted, and then probed with affinity-purified anti–ZYG-9 antibodies. A band of 155 kD, the predicted size of the ZYG-9 protein, was detected in wild-type embryos (*N2*) and in the temperature-sensitive *zyg-9* allele *b244*, but was not detected in the strong alleles *b279*, *b301*, *it3,* and *it152* or in the temperature-sensitive allele *b288*. Antibodies against α-tubulin provide a loading control.

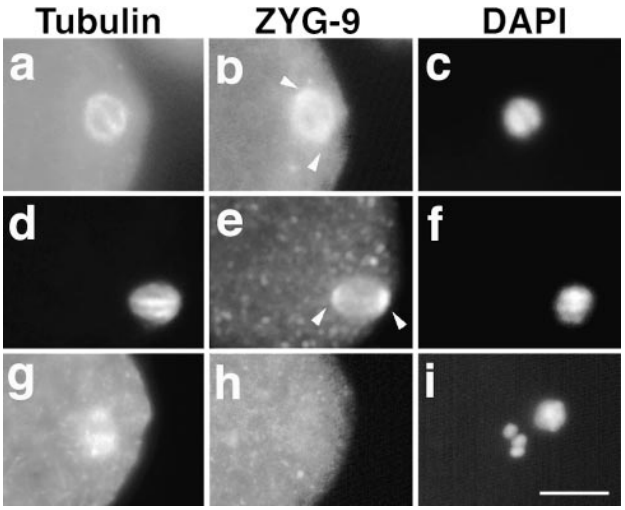


*Figure 6.* Distribution of ZYG-9 during meiosis. Immunofluorescence micrographs of wild-type *(a–f)* and *zyg-9 (it3)* mutant embryos *(g–h)* fixed and labeled with anti–α-tubulin antibodies (*left column*), anti-ZYG-9 (*middle column*), and DAPI (*right column*). *(a–c)* Early metaphase I. *(d–f)* Late metaphase I. *(a* and *d)* Tubulin is detected throughout the spindle but is not noticeably concentrated at the poles. *(b* and *e)* ZYG-9 is detected throughout the spindle and at polar regions not obviously occupied by microtubules (*arrows*). *(g–i)* Meiotic stage embryos of the strong *zyg-9* mutant *it3*. Note the disorganized spindle *(g),* absence of ZYG-9 staining *(h)*, and abnormal chromosome configuration *(i)*. Bar, 10 μm.

metaphase spindle (Fig. 6, *b* and *e*). This localization pattern is similar, but not identical to that of tubulin (Fig. 6, *a*, *b*, *d,* and *e*). ZYG-9 appears more concentrated than tubulin at the spindle poles (*arrows*) and more diffuse in the central spindle. This distribution persists through anaphase with a progressive decrease in the relative strength of the signal from the central spindle (data not shown).

### *Mitosis*

After the second meiotic division, ZYG-9 localizes to two small spots adjacent to the male pronucleus (Fig. 7 *b*). Embryos at this stage costained with antitubulin antibodies revealed that these spots correspond to the foci of the astral microtubules (Fig. 7 *a*). This localization pattern suggests that ZYG-9 is a component of the centrosome. We were unable to compare the spatial and temporal distribution of ZYG-9 to the distribution of known centrosomal proteins such as γ-tubulin (Stearns et al., 1991) or pericentrin (Doxsey et al., 1994), because available antibodies did not cross-react with *C. elegans* proteins or reacted with proteins that were not specifically localized to the centrosomes.

ZYG-9 protein localizes to the centrosomes throughout the first mitosis, but is also detected in the central mitotic spindle region between late prometaphase and early anaphase (Fig. 7, *e* and *h*). Between telophase and interphase, ZYG-9 staining at the centrosome becomes increasingly diffuse (Fig. 7 *n*) and is eventually undetectable (data not shown). ZYG-9 protein exhibits the same distribution pattern in all mitotic cells of the developing embryo (Fig. 8 *a*), in mitotic cells of the gonad (Fig. 8 *c*), and in dividing spermatocytes (data not shown). The level of ZYG-9 protein in the cytoplasm appears to be reduced in mitotic cells as compared with interphase cells suggesting that the ZYG-9 protein may be cycling between the centrosome and cytoplasm in a cell cycle-dependent manner (Fig. 8 *a*).

To determine whether the localization of ZYG-9 proteins to the centrosome was dependent upon microtubules, we treated cells with nocodazole before immunostaining for ZYG-9 and tubulin. Under our experimental conditions (refer to Materials and Methods) meiotic and mitotic spindle microtubules, including astral microtubules, were undetectable in most cells after nocodazole treatment, although a small amount of tubulin staining was present at the centrosome (Fig. 9 *a*). Under these conditions, significant amounts of ZYG-9 protein were detected at centrosomes (Fig. 9 *b*). These results suggest that long microtubules are not required to maintain ZYG-9 at the centrosome. It is likely, therefore, that ZYG-9 is an integral component of the centrosome rather than a constituent transported there along microtubules. However, because we were unable to completely eliminate tubulin from the centrosomes, we cannot rule out the possibility that tubulin or short microtubules are required for centrosomal localization of ZYG-9.

These experiments also revealed that spindle disassembly led to an accumulation of ZYG-9 in the region of the chromosomes in both mitotic and meiotic cells (Fig. 9, *b*, *e*, and *h*). In meiotic cells, the protein forms a halo around individual bivalents (Fig. 9 *h*), whereas in mitotic cells the protein exhibits a more diffuse distribution (Fig. 9 *b*).

It appears that this accumulation around chromatin is not a passive consequence of spindle disassembly. Treatments of one-cell embryos with nocodazole before pronuclear migration can result in *zyg-9* phenocopies in which pronuclear migration fails and the mitotic apparatus forms in the posterior and includes only the paternal chromosomes (Albertson et al., 1984). We observed that in such embryos (Fig. 9, *d–f*), ZYG-9 accumulated not only around the paternal chromosomes that had been incorporated into the spindle apparatus before its disassembly (Fig. 9 *e*, *small arrow*), but also around the condensed chromosomes of the female pronucleus that had never associated with the spindle (Fig. 9 *e*, *large arrow*). Because

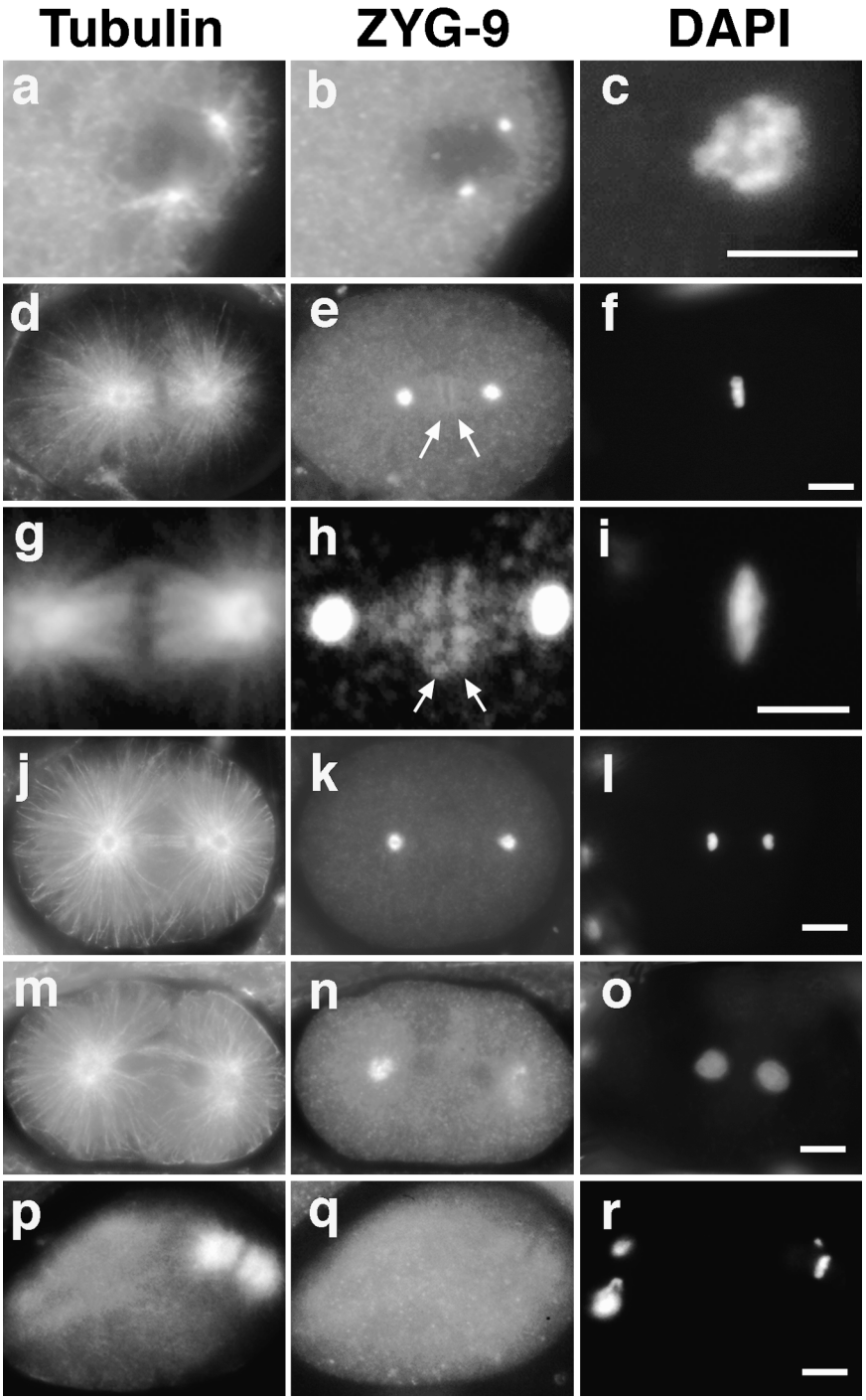


*Figure 7.* ZYG-9 distribution during the first mitosis. Immunofluorescence micrographs of wild-type *(a–o)* and *zyg-9 (it3)* mutant embryos *(p–r)* fixed and labeled with anti–α-tubulin antibodies (*left column*), anti-ZYG-9 antibodies (*middle column*), and DAPI (*right column*). ZYG-9 is first detected as two brightly staining dots adjacent to the male pronucleus *(b)*. The location of these spots corresponds to the location of the newly duplicated centrosomes *(a)*. Protein is detected at the spindle poles through anaphase *(e, h,* and *k)*, but becomes diffuse at late telophase *(n)*. During metaphase *(e* and *h;* two different embryos) and early anaphase (data not shown), ZYG-9 is also detected in the central spindle region (*arrows*). At the central spindle of a metaphase stage embryo (*h*; enlarged and contrast-enhanced to show detail), ZYG-9 is detected in the kinetochore region. *(g–i)* ZYG-9 protein is not detected in mitotic cells of *zyg-9* (*it3*) embryos *(q)*. The DAPI-stained bodies at the right in panel *r* are polar bodies and an abnormal female pronucleus. Bar, 10 μm.



we saw a similar distribution of ZYG-9 protein around the dispersed chromosomes in the disorganized meiotic spindles of *mei-1* mutant embryos (see below and Fig. 9 *j*), we believe that the localization pattern observed in nocodazole-treated embryos is not the result of nonspecific effects of nocodazole.

### *ZYG-9 Distribution Is Affected by Loss of Function, but Not Gain of Function, Mutations in mei-1*

The distribution of ZYG-9 within the meiotic spindle is similar to that of MEI-1, an ATPase required for meiotic spindle formation (Mains et al., 1990*b*; Clark-Maguire and Mains, 1994*a*,*b*). In *mei-1* loss of function mutant embryos, meiotic spindles do not form or are disorganized, but mitotic spindles function normally. A gain of function *mei-1* mutation (*ct46*) and a gain of function mutation in another gene, *mel-26(ct61),* do not affect meiosis but lead to mislocalization of the MEI-1 protein to the microtubules and centrosomes of the mitotic spindle and produce a Zyg-9–like phenotype (Mains et al., 1990*a*; Clark-Maguire and Mains, 1994*b*). To better understand the relationship between ZYG-9 and MEI-1, we studied the distribution of ZYG-9 protein in the mitotic spindles of gain of function

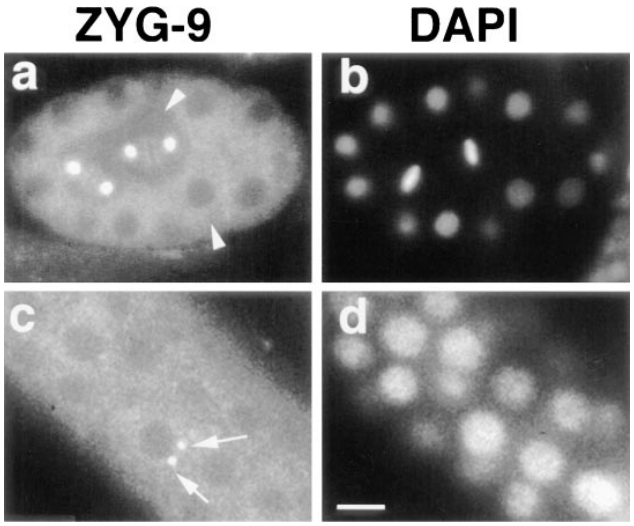


*Figure 8.* ZYG-9 distribution in later stage embryos *(a* and *b)* and in adult gonads *(c* and *d)* stained with ZYG-9 antibodies (*left column*) and DAPI (*right column*). ZYG-9 distributes to the centrosome and central spindle region in mitotic cells throughout embryogenesis and in mitotic cells of the gonad. (*a*) *Arrowheads;* location of a metaphase and an interphase cell for comparison. Note the relatively high concentration of ZYG-9 in the cytoplasm of interphase cells relative to mitotic cells. (*c*) *Arrows;* ZYG-9 staining in centrosomes of a cell just entering mitosis in an adult gonad. Bar, 10 μm.

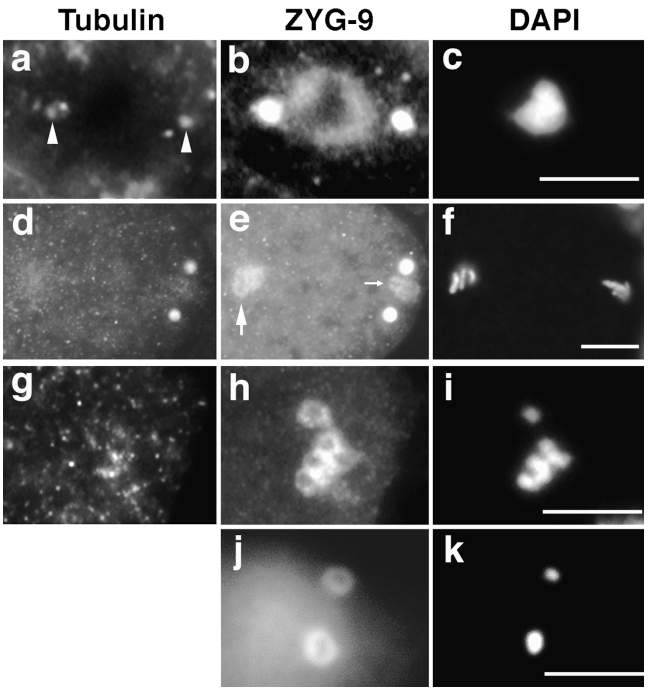


*Figure 9.* Distribution of ZYG-9 protein after the disruption of microtubules by nocodazole. Immunofluorescence micrographs of wild-type embryos treated with nocodazole, fixed, and then labeled with anti–α-tubulin antibodies (*left column*), anti–ZYG-9 antibodies (*middle column*), and DAPI (*right column*). *(a–c)* In mitotic stage embryonic cells, spindle microtubules are disrupted although weak tubulin staining is still detected at the centrosome (see *a, arrowheads*). ZYG-9 is detected at the centrosomes *(b)* and in the region surrounding the chromosomes. *(d–f)* A one-cell embryo treated with nocodazole before pronuclear migration. ZYG-9 accumulates at the sperm-derived centrosomes (*e*, *right*, *bright dots*) and around the paternal chromosomes (*small arrow*) and condensed chromosomes of the female pronucleus (*large arrow*). *(g–i)* Meiotic-stage embryos treated with nocodazole. Spindle microtubules are undetectable *(g)*. ZYG-9 localizes around individual meiotic chromosomes *(h)*. *(j* and *k)* ZYG-9 localizes around the widely dispersed meiotic chromosomes in the disorganized meiotic spindles of *mei-1* mutants. Bar, 10 μm.

and loss of function *mei-1* mutant embryos. In *mei-1(ct46)* gain of function embryos, the distribution of ZYG-9 appeared normal during both meiotic and mitotic stages indicating that the presence of MEI-1 protein in the mitotic spindle does not prevent the association of ZYG-9. A decrease in the quantity of ZYG-9 protein at the poles, however, might not have been detected in this analysis. In *mei-1*(*ct46ct101*) loss of function mutant embryos, in which no meiotic spindle forms, the ZYG-9 protein was found to accumulate around meiotic chromosomes (Fig. 9, *j* and *k*), similar to its distribution after nocodazole treatment.

## *Discussion*

The *zyg-9* mutant phenotypes of failure in both pronuclear migration and spindle rotation have been interpreted as direct consequences of the observed decrease in microtubule length (Albertson, 1984; Kemphues et al., 1986). Our results, together with the *zyg-9* mutant phenotype, lead us to propose that ZYG-9 functions within the spindle apparatus during early embryogenesis to increase the length of the microtubules. Such a role would be required for generating the exceptionally long microtubules necessary for cell division and spindle positioning in the large blastomeres of the early embryo. Because meiotic spindles, which do not require long microtubules, are also disorganized in *zyg-9* mutants, the protein must also have some role in spindle organization. Based on available data, we propose two models for *zyg-9* action.

Our observation that ZYG-9 protein localizes predominantly to the spindle poles suggests that it may influence microtubule length by affecting microtubule stability at the spindle poles. In this model, ZYG-9 antagonizes other constitutively present centrosomal factors that normally facilitate microtubule disassembly at the minus ends. Such factors have been described; microtubule-severing ATPases have been identified in *Saccharomyces purpuratus* (McNally and Vale, 1993) and *Xenopus* eggs (Vale, 1991), and the *S. purpuratus* protein has been shown to localize to the centrosome (McNally et al., 1996). The *S. cerevisiae* kinesin-like motor protein, Kar3p, which localizes to the spindle poles of the preanaphase spindle, is thought to depolymerize or otherwise destabilize microtubules during vegetative growth (Saunders et al., 1997).

The meiotic defects associated with *zyg-9* mutations indicate that ZYG-9 protein is also essential for meiotic spindle organization and function. The pattern of ZYG-9 localization during meiosis is consistent with this role, but it is paradoxical that a protein required to produce long astral microtubules would also be essential for the organization of the very short meiotic spindle. One possible recon-

ciliation of the two phenotypes is that the activity of ZYG-9 is required to counterbalance the activity of a factor that acts to limit the length of meiotic spindle microtubules. One candidate for such a factor is the MEI-1 ATPase. This protein is required for spindle assembly, exhibits a pattern of localization in the meiotic spindle which is similar to that of ZYG-9 and results in the formation of short microtubules when mislocalized to the mitotic spindle by gain of function mutations (Mains et al., 1990*b*; Clark-Maguire and Mains, 1994*a*,*b*). Our observation that mitotic ZYG-9 protein is not displaced by MEI-1 protein in gain of function *mei-1* mutants indicates that if the two proteins do act antagonistically, they probably do not do so by competing for a common anchoring site.

An alternative model for ZYG-9 function is suggested by the finding that ZYG-9 localizes to the region surrounding chromosomes as well as to centrosomes and that this localization is enhanced after nocodazole treatment. One interpretation of this distribution that is consistent with the meiotic spindle defect is that ZYG-9 functions in chromosome-mediated spindle organization. Several studies have shown that, in the absence of centrosomes, spindle microtubules form and elongate in the region surrounding chromatin and are subsequently reorganized into a bipolar array with microtubule minus ends focused at the spindle poles (for review see Hyman and Karsenti, 1996). ZYG-9 is not required for the nucleation of microtubules in the meiotic spindle, since disorganized arrays of microtubules are detected around meiotic chromosomes in strong *zyg-9* alleles (Mains et al., 1990*b*). This protein may be recruited to the region surrounding the meiotic chromosomes, however, where it, along with other proteins, promotes the elongation and rearrangement of microtubules into an ordered bipolar array.

The progressive accumulation of ZYG-9 protein at the poles of the meiotic spindle is consistent with such a role. Interestingly, the distribution pattern of γ-tubulin in the *Xenopus* meiotic spindles exhibits certain similarities to the distribution of ZYG-9 during meiosis (Gard et al., 1995). γ-Tubulin associates with the minus ends of microtubules and has been shown to play a role in microtubule nucleation (Li and Joshi, 1995; Zheng et al., 1995). During the early stages of meiosis in *Xenopus* embryos, γ-tubulin surrounds meiotic chromosomes. By metaphase, it localizes within meiotic spindles and is enriched at poles. Finally, at late stages of meiosis, γ-tubulin is present primarily at the spindle poles (Gard et al., 1995). It has been suggested that this changing pattern of γ-tubulin distribution in the meiotic spindle may reflect the proposed reorganization of the minus ends of microtubules into the spindle poles (Gard et al., 1995).

Although we have shown that ZYG-9 localizes to the mitotic apparatus throughout embryogenesis and is present in the centrosomes of mitotic germ line cells, genetic data indicates that this protein is essential only during early embryogenesis (Kemphues et al., 1986; Mains et al., 1990*a*). One interpretation of these observations is that ZYG-9 activity is only necessary for the elongation of microtubules in the relatively large cells of the early embryo. After the onset of gastrulation, ZYG-9 may be inactive, or active but functionally redundant.

The relationship between ZYG-9 and the microtubule-associated proteins ch-TOG, $p93^{Dis1}$, and Stu2p remains to be determined. Interestingly, like ZYG-9, ch-TOG (Charrasse et al., 1998), $p93^{Dis1}$ (Nabeshima et al., 1995), and Stu2p (Wang and Huffaker, 1997) all localize to the spindle poles. In addition, the localization of ch-TOG (Charrasse et al., 1998), and $p93^{Dis1}$ (Nabeshima et al., 1995), like ZYG-9, is cell cycle dependent. As the sequence similarity among these proteins is restricted to a domain of 220 amino acids, it is possible that this region is involved in the localization of these proteins to the spindle poles. However, Nakaseko et al. (1996) have shown that the carboxy-terminal region of $p93^{Dis1}$, which does not include the conserved domain, is necessary and sufficient for localization of this protein to the spindle poles. Interestingly, truncated $p93^{Dis1}$ proteins lacking the amino-terminal region, including the conserved domain, localize to the spindle poles throughout the cell cycle, suggesting that the conserved domain may play a role in cell cycle–dependent changes in the localization of $p93^{Dis1}$ protein (Nakaseko et al., 1996). Perhaps this domain has a similar function in ZYG-9 and ch-TOG. The identification of the components of the centrosome and chromosomes with which ZYG-9 interacts may provide further insight into the function of ZYG-9 in regulating microtubule organization.

The authors thank A. Coulson and J. Sulston (both from Sanger Centre, Cambridge, UK) for cosmid strains, and Y. Kohara for providing the cDNA clone yk28d8. Some genetic strains were provided by the Caenorhabditis Genetics Center, which is supported by the National Institutes of Health [NIH] National Center for Research Resources, Bethesda, MD).

This work was supported by a NIH grant (HD27689), a Cornell University Sigma XI grant in Aid of Research, a Mario Enoudi grant for International Studies, and a Bourse Chateaubriand Fellowship from the Department of Science and Technology of The Embassy of France (Washington, D.C.).

Received for publication 10 December 1997 and in revised form 17 April 1998.

### *References*

Albertson, D. 1984. Formation of the first cleavage spindle in nematode embryos. *Dev. Biol.* 101:61–72.

Altschul, S.F., W. Gish, W. Miller, E.W. Myers, and D.J. Lipman. 1990. Basic local alignment search tool. *J. Mol. Biol.* 215:403–410.

Andersen, S.S.L., and E. Karsenti. 1997. XMAP310: A *Xenopus* rescue-promoting factor localized to the mitotic spindle. *J. Cell Biol.* 139:975–983.

Andersen, S.S., B. Buendia, J.E. Dominguez, A. Sawyer, and E. Karsenti. 1994. Effect on microtubule dynamics of XMAP230, a microtubule-associated protein present in *Xenopus laevis* eggs and dividing cells. *J. Cell Biol.* 127: 1289–1299.

Ausubel, F.M., R. Brent, R.E. Kingston, J.G. Seidman, J.A. Smith, and K. Struhl. 1995. Current Protocols in Molecular Biology. V.B. Chanda, editor. John Wiley & Sons, Inc, New York.

Charrasse, S., M. Mazel, S. Taviaux, P. Berta, T. Chow, and C. Larroque. 1995. Characterization of the cDNA and pattern of expression of a new gene overexpressed in human hepatomas and colonic tumors. *Eur. J. Biochem.* 234: 406–413.

Charrasse, S., M. Schroeder, C. Gauthier-Rouviere, F. Ango, L. Cassimeris, D.L. Gard, and C. Larroque. 1998. The TOGp protein is a new human microtubule associated protein homologous to the *Xenopus* XMAP215. *J. Cell Sci.* 111:1371–1383.

Clark-Maguire, S., and P.E. Mains. 1994*a*. *mei-1*, a gene required for meiotic spindle formation in *Caenorhabditis elegans*, is a member of a family of ATPases. *Genetics*. 136:533–546.

Clark-Maguire, S., and P.E. Mains. 1994*b*. Localization of the *mei-1* gene product of *Caenorhabditis elegans*, a meiotic-specific spindle component. *J. Cell Biol.* 126:199–209.

Collins, J., E. Forbes, and P. Anderson. 1989. The Tc3 family of transposable genetic elements in *Caenorhabditis elegans*. *Genetics*. 121:47–55.

Doxsey, S.J., P. Stein, L. Evans, P.D. Calarco, and M. Kirschner. 1994. Pericentrin, a highly conserved centrosome protein involved in microtubule organization. *Cell*. 76:639–650.

Draper, B.W., C.C. Mello, B. Bowerman, J. Hardin, and J.R. Priess. 1996. MEX-3 is a KH domain protein that regulates blastomere identity in early *C. elegans* embryos. *Cell*. 87:205–216.

Durbin, R.M., and J.T. Thierry-Mieg. 1991. A *C. elegans* database (ACeDB). *FTP://ncbi.nlm.nih.gov/repository/ACeDB*.

Gard, D.L., and M.W. Kirschner. 1987. A microtubule-associated protein from *Xenopus* eggs that specifically promotes assembly at the plus-end. *J. Cell Biol*. 105:2203–2215.

Gard, D.L., B.J. Cha, and M.M. Schroeder. 1995. Confocal immunofluorescence microscopy of microtubules, microtubule-associated proteins, and microtubule-organizing centers during amphibian oogenesis and early development. *Curr. Top. Dev. Biol*. 31:383–431.

Guo, S., and K.J. Kemphues. 1995. *par-1*, a gene required for establishing polarity in *C. elegans* embryos, encodes a putative Ser/Thr kinase that is asymmetrically distributed. *Cell*. 8145:611–620.

Harlow, E., and D.P. Lane. 1988. Antibodies: A Laboratory Manual. Cold Spring Harbor Laboratory Press, Cold Spring Harbor, New York. 726 pp.

Hunter, C.P., and C. Kenyon. 1996. Spatial and temporal controls target pal-1 blastomere-specification activity to a single blastomere lineage in *C. elegans* embryos. *Cell*. 87:217–226.

Hyman, A.A., and E. Karsenti. 1996. Morphogenetic properties of microtubules and mitotic spindle assembly. *Cell*. 84:401–410.

Kemphues, K.J., N. Wolf, W.B. Wood, and D. Hirsh. 1986. Two loci required for cytoplasmic organization in early embryos of *Caenorhabditis elegans*. *Dev. Biol.* 113:449–460.

Kemphues, K.J., M. Kusch, and N. Wolf. 1988. Maternal-effect lethal mutations on linkage group II of *Caenorhabditis elegans*. *Genetics*. 120:977–986.

Li, Q., and H.C. Joshi. 1995. Gamma-tubulin is a minus end-specific microtubule-binding protein. *J. Cell Biol.* 131:207–214.

Lin, R., S. Thompson, and J.R. Priess. 1995. pop-1 encodes an HMG box protein required for the specification of a mesoderm precursor in early *C. elegans* embryos. *Cell*. 83:599–609.

Mains, P.E., I. Sulston, and W.B. Wood. 1990*a*. Dominant maternal-effect mutations causing embryonic lethality in *Caenorhabditis elegans*. *Genetics*. 125: 351–369.

Mains, P.E., K.J. Kemphues, S.A. Sprunger, I.A. Sulston, and W.B. Wood. 1990*b*. Mutations affecting the meiotic and mitotic divisions of the early *Caenorhabditis elegans* embryo. *Genetics*. 126:593–605.

McNally, F.J., and R.D. Vale. 1993. Identification of katanin, an ATPase that severs and disassembles stable microtubules. *Cell*. 75:419–429.

McNally, F.J., K. Okawa, A. Iwamatsu, and R.D. Vale. 1996. Katanin, the microtubule-severing ATPase, is concentrated at centrosomes. *J. Cell Sci*. 109: 561–567.

Mello, C.C., J.M. Kramer, D. Stinchcomb, and V. Ambros. 1991. Efficient gene transfer in *C. elegans*: Extrachromosomal maintenance and integration of transforming sequences. *EMBO (Eur. Mol. Biol. Organ.) J.* 10:3959–3970.

Mello, C.C., C. Schubert, B. Draper, W. Zhang, R. Lobel, and J.R. Priess. 1996. The PIE-1 protein and germline specification in *C. elegans* embryos. *Nature*. 382:710–712.

Nabeshima, K., H. Kurooka, M. Takeuchi, K. Kinoshita, Y. Nakaseko, and M. Yanagida. 1995. $p93^{Dis1}$, which is required for sister chromatid separation, is a novel microtubule and spindle pole body-associating protein phosphorylated at the Cdc2 target sites. *Genes Dev*. 9:1572–1585.

Nakaseko, Y., K. Nabeshima, K. Kinoshita, and M. Yanagida. 1996. Dissection of fission yeast microtubule associating protein $p93^{Dis1}$: regions implicated in regulated localization and microtubule interaction. *Genes Cells*. 1:633–644.

Ohkura, H., Y. Adachi, N. Kinoshita, O. Niwa, T. Toda, and M. Yanagida. 1988. Cold-sensitive and caffeine-supersensitive mutants of the *Schizosaccharomyces pombe* dis genes implicated in sister chromatid separation during mitosis. *EMBO (Eur. Mol. Biol. Organ.) J.* 7:1465–1473.

Okkema, P.G., and A. Fire. 1994. The *Caenorhabditis elegans* NK-2 class homeoprotein CEH-22 is involved in combinatorial activation of gene expression in pharyngeal muscle. *Development (Camb.)*. 120:2175–2186.

Rocheleau, C.E., W.D. Downs, R. Lin, C. Wittmann, Y. Bei, Y.H. Cha, M. Ali, J.R. Priess, and C.C. Mello. 1997. Wnt signaling and an APC-related gene specify endoderm in early *C. elegans* embryos. *Cell*. 90:707–716.

Sanger, F., S. Nicklen, and A.R. Coulson. 1977. DNA sequencing with chain-terminating inhibitors. *Proc. Natl. Acad. Sci. USA*. 74:5463–5467.

Saunders, W., D. Hornack, V. Lengyel, and C. Deng. 1997. The *Saccharomyces cerevisiae* kinesin-related motor Kar3p acts at preanaphase spindle poles to limit the number and length of cytoplasmic microtubules. *J. Cell Biol*. 137: 417–431.

Stearns, T., L. Evans, and M. Kirschner. 1991. Gamma-tubulin is a highly conserved component of the centrosome. *Cell*. 65:825–836.

Stewart-Savage, J., and R.D. Grey. 1982. The temporal and spatial relationships between cortical contraction, sperm trail formation, and pronuclear migration in fertilized eggs of *Xenopus laevis*. *Wilhelm Roux's Arch. Dev. Biol.* 191:241–245.

Vale, R.D. 1991. Severing of stable microtubules by a mitotically activated protein in *Xenopus* egg extracts. *Cell*. 64:827–839.

Vasquez, R.J., D.L. Gard, and L. Cassimeris. 1994. XMAP from *Xenopus* eggs promotes rapid plus end assembly of microtubules and rapid microtubule polymer turnover. *J. Cell Biol.* 127:985–993.

Verde, F., M. Dogterom, E. Stelzer, E. Karsenti, and S. Leibler. 1992. Control of microtubule dynamics and length by cyclin A– and cyclin B–dependent kinases in *Xenopus* egg extracts. *J. Cell Biol*. 118:1097–1108.

Wang, P.J., and T.C. Huffaker. 1997. Stu2p: A microtubule-binding protein that is an essential component of the yeast spindle pole body. *J. Cell Biol*. 139: 1271–1280.

Waterston, R., and J. Sulston. 1995. The genome of *Caenorhabditis elegans*. *Proc. Natl. Acad. Sci. USA*. 92:10836–10840.

Williams, B.D., B. Schrank, C. Huynh, R. Shownkeen, and R.H. Waterston. 1992. A genetic mapping system in *Caenorhabditis elegans* based on polymorphic sequence-tagged sites. *Genetics*. 131:609–624.

Wood, W.B., R. Hecht, S. Carr, R. Vanderslice, N. Wolf, and D. Hirsh. 1980. Parental effects and phenotypic characterization of mutations that affect early development in *Caenorhabditis elegans*. *Dev Biol*. 74:446–469.

Zheng, Y., M.L. Wong, B. Alberts, and T. Mitchison. 1995. Nucleation of microtubule assembly by a gamma-tubulin-containing ring complex. *Nature*. 378:578–583.